

# High-dimensional Bayesian Optimization for CNN Auto Pruning with Clustering and Rollback

Jiandong Mu,<sup>1</sup> Hanwei Fan,<sup>1</sup> Wei Zhang,<sup>1</sup>

<sup>1</sup> The Hong Kong University of Science and Technology (HKUST), China

jmu@connect.ust.hk, hfanah@connect.ust.hk, wei.zhang@ust.hk

## Abstract

Pruning has been widely used to slim convolutional neural network (CNN) models to achieve a good trade-off between accuracy and model size so that the pruned models become feasible for power-constrained devices such as mobile phones. This process can be automated to avoid the expensive hand-crafted efforts and to explore a large pruning space automatically so that the high-performance pruning policy can be achieved efficiently. Nowadays, reinforcement learning (RL) and Bayesian optimization (BO)-based auto pruners are widely used due to their solid theoretical foundation, universality, and high compressing quality. However, the RL agent suffers from long training times and high variance of results, while the BO agent is time-consuming for high-dimensional design spaces. In this work, we propose an enhanced BO agent to obtain significant acceleration for auto pruning in high-dimensional design spaces. To achieve this, a novel clustering algorithm is proposed to reduce the dimension of the design space to speedup the searching process. Then, a roll-back algorithm is proposed to recover the high-dimensional design space so that higher pruning accuracy can be obtained. We validate our proposed method on ResNet, MobileNet, and VGG models, and our experiments show that the proposed method significantly improves the accuracy of BO when pruning very deep CNN models. Moreover, our method achieves lower variance and shorter time than the RL-based counterpart.

## 1 Introduction

Convolutional neural networks (CNN) are becoming popular due to their high performance and universality. There is a growing trend to apply CNNs in different scenarios such as object detection, speech recognition, *etc.* However, the high performance of CNNs is at the expense of their large model size and high computing complexity, which have prevented it from having a broader usage. To solve this problem, network pruning (Han et al. 2015) has been proposed to reduce the model size with little accuracy loss. Many works, *e.g.*, (He et al. 2017; Zhuang et al. 2018; Louizos et al. 2017) have been proposed to prune CNNs with different granularity. Among these works, channel pruning, which reduces the model size and computing complexity by removing the re-

dundant channels on the feature map, is widely adopted due to its high efficiency in hardware implementation.

As the depth of CNN models rapidly increases, the design space of the pruning policies, which indicates the preservation ratio of each layer of the CNN model, becomes too large for the heuristic method to explore efficiently. The extra hand-crafted efforts required in the pruning process may diminish the benefit that it has brought, making pruning less attractive. To reduce the manpower overhead introduced by the pruning process while exploring a larger pruning space, RL-based automatic model compression (AMC) (He et al. 2018) was proposed to automate the channel pruning process. However, the RL-based method leads to a large time overhead as massive data and training trials are needed for the RL agent to converge. To increase the practicality of auto pruning, a better agent is expected to be applied to search the design space more efficiently.

Bayesian optimization (BO) (Mockus, Tiesis, and Zilinskas 1978) is known to be an effective method to tune the hyper-parameters for the black-box function with a small computational budget due to its high sample efficiency. However, BO suffers from a fatal drawback that the efficiency of BO drops significantly when dealing with high-dimensional problems. As a result, it would be challenging to directly apply BO to compress very deep networks. Currently, to maintain high efficiency, the BO-based pruning framework is usually used to deal with shallow networks.

In this work, observing that layers with similar structures have similar redundancy, we propose to cluster the layers and share the same preservation ratio within a cluster so that the parameters to be tuned in the BO agent can be significantly reduced and the searching efficiency can be greatly improved with little loss in accuracy. However, the decrease in searching time is at the expense of missing the optimal pruning policy since we reduce the design space by assuming that similar layers can share the same preservation ratio. To solve this problem, we propose a rollback scheme in which we recover the GP model back into the high-dimensional space and perform a fine-grained search with the low-dimensional data as the prior knowledge. In addition, to fully utilize the information collected during the policy searching in low-dimensional space, we propose an adaptive feasible region scaling scheme to reduce the workload of the BO agent after rollback and to achieve a faster

fine-grained search.

In summary, we make the following contributions:

- We propose to solve the high-dimensional problem with a clustering-based dimension reduction scheme to reduce the tuning variables so that the BO agent can prune the CNN model efficiently.
- A rollback mechanism is used to recover the high-dimensional space so that the optimal pruning policy won't be missed and the accuracy of the pruned model can be further improved.
- Our experiments show that our methods can explore the design space with a considerable improvement in accuracy than naive BO agent while have little running time overhead. In the ResNet56 experiments, our method delivers a 2.2% higher accuracy. For challenging tasks like pruning MobileNet V1 and V2 on Imagenet, our method achieves a 1.8% and 1.6% higher accuracy, respectively. All the above results also outperform the RL-based counterparts in both accuracy and running time.

## 2 Related Works

### 2.1 Reinforcement Learning based Auto Pruning

In (He et al. 2018), the authors employ a deep deterministic policy gradient (DDPG) agent (Lillicrap et al. 2015), which is one of the most popular RL algorithms for continuous action spaces, to automatically generate the optimal pruning policy for channel pruning, so that human efforts can be released from the tedious handcrafting work. In (Wang et al. 2019), this RL-based auto pruning scheme is further extended to model quantization for the first time. However, the RL agent is still time-consuming since it needs hundreds of trials to interact with the environments, which in this case is channel pruning and accuracy measurement, to train the actor network and critic network inside it. Therefore, it is of great interest to develop a novel auto pruning agent or improve the convergence speed of the RL agent.

### 2.2 Bayesian Optimization-based Auto Pruning

BO is an optimization framework that employs a probabilistic model to predict the performance and variation of the design space so that the efficiency of the next sample can be maximized. The probabilistic model will be continually updated during the sampling process. Nowadays, BO is widely used to tune hyperparameters due to its high sample efficiency. Therefore, it becomes a natural thought to apply BO to CNN pruning. A few works (Ma et al. 2019; Tung, Muralidharan, and Mori 2017; Chen et al. 2018) on automatically pruning CNN based on a BO agent are introduced here. In (Tung, Muralidharan, and Mori 2017), the author proposed a fine-pruning method, which applied a BO agent to automatically adapt the layer-wise pruning parameters over time as the network changes. The work in (Chen et al. 2018) further improves this framework by setting constraints on BO and designing a cooling scheme to gradually prune the CNN model to a user-specified pruning ratio.

However, these works dismiss the curse of high dimensionality of BO as they only conduct experiments on shallow

variable	meaning
$i$	index of layer
$n$	number of input channels for layer
$k$	kernel size
$c, c'$	number of output channels before/after pruning
$\Theta, \Theta'$	network model before/after pruning
$p_i$	preservation ratio for layer $i$
$\mathbf{P}$	pruning policy for the model
$p_t$	target preservation ratio
$N$	number of layers of the network

Table 1: Variables in this work.

networks such as AlexNet (Krizhevsky, Sutskever, and Hinton 2012) which has only eight layers. In (Ma et al. 2019), the authors successfully apply BO to prune deep networks, *e.g.*, VGG16 (Simonyan and Zisserman 2014), ResNet50 (He et al. 2016), *etc.*, with an efficient acquisition function and a fast quality measure of the sampled network. However, the high-dimensional problem in the BO agent is not fundamentally solved and the computing workload becomes prohibitive if the depth of the network further grows. In (Wang et al. 2013), the author proposed to solve the high-dimensional problem by mapping it to an efficient subspace via random embeddings. However, the effectiveness of the proposed algorithm is bounded by the rank of the subspace. In CNN pruning, the preserve ratio of each layer is independent, therefore, it's hard to map the high-dimensional space to a low rank subspace via random embeddings.

In this work, we propose a clustering-based BO agent to reduce the dimensionality of the auto pruning problem, which is then followed by a rollback algorithm to fine-tune the accuracy so that the curse of dimensionality can be resolved fundamentally.

## 3 Methodology

In this section, we introduce our methodology by forming the auto pruning task as a BO process. Before revealing the details, we list the frequently used variables in Table 1.

### 3.1 Channel Pruning with Bayesian Optimization

In this work, we mainly focus on channel pruning as it can achieve a good trade-off between model size and accuracy while being hardware-friendly. We adopt the channel pruning scheme in (He et al. 2017) to prune the neural network. However, our proposed framework also works for other pruning schemes. In channel pruning, a weights tensor with the shape of  $n \times c \times k \times k$  is pruned into  $n \times c' \times k \times k$ ; therefore, the preservation ratio  $p$  is  $c'/c$ . Then, the problem becomes determining the optimal  $p_i$  for layer  $i$  to maximize the accuracy of the pruned network while satisfying the constraints. This can be formulated as the following optimization problem:

$$\begin{aligned}
 & \max_{\mathbf{P}} f(\Theta') \\
 & \text{s.t. } p_f \leq p_t \\
 & \Theta' = \text{Pruning}(\Theta, \mathbf{P}) \\
 & p_f = \text{Flops}(\Theta')/\text{Flops}(\Theta),
 \end{aligned} \tag{1}$$

where the *Pruning* and *Flops* functions are well-defined functions and can be implemented explicitly in the program.  $f$  is the target function, which is usually a black-box function. In our case, it is the accuracy of the pruned network and can be measured by conducting inferences on the images in the validation set.

This problem turns out to be hard to solve since there is no explicit form of  $f$  due to the complex relationship between channel pruning policy and the corresponding accuracy. An alternative method is to build a fast model to approximate the black box function  $f$  by iteratively interacting with the channel pruner and the optimal pruning policy  $\mathbf{P}^*$  can be achieved by finding the maximum value of the model. BO, which models the black-box function with a continually updated probabilistic model, *e.g.* Gaussian process model (Mockus and Mockus 1991), becomes promising for optimizing expensive black-box functions due to its high sample efficiency and favorable statistical properties.

During the BO process, we note the sampled policy in the  $t$ th round as  $\mathbf{P}_t \in \mathbb{R}^N$ , where  $N$  is the depth of the neural network. Similarly, the pruning policies for time 1 to  $t$  can be noted as  $\mathbf{P}_{1:t}$ . As we have mentioned before, we assume that the pruning samples can be modeled as a Gaussian process and therefore we have

$$f(\Theta, \mathbf{P}_{1:t}) \sim \mathcal{N}(\mathbf{m}(\mathbf{P}_{1:t}), \mathbf{K}(\mathbf{P}_{1:t}, \mathbf{P}_{1:t})), \quad (2)$$

where  $\mathbf{m}$  is the mean function, and  $\mathbf{K}(\mathbf{P}_{1:t}, \mathbf{P}_{1:t})$  is the variance matrix. In the following discussion, we denote  $f(\Theta, \mathbf{P}_{1:t})$  by  $f(\mathbf{P}_{1:t})$  for simplicity. Then, the joint distribution of the previous samples together with the next sample can be represented by

$$\begin{bmatrix} f(\mathbf{P}_{1:t}) \\ f(\mathbf{P}_{t+1}) \end{bmatrix} \sim \mathcal{N} \left( \begin{bmatrix} \mathbf{m}(\mathbf{P}_{1:t}) \\ \mathbf{m}(\mathbf{P}_{t+1}) \end{bmatrix}, \begin{bmatrix} \mathbf{K}(\mathbf{P}_{1:t}, \mathbf{P}_{1:t}), \mathbf{k}(\mathbf{P}_{1:t}, \mathbf{P}_{t+1}) \\ \mathbf{k}(\mathbf{P}_{t+1}, \mathbf{P}_{1:t}), \mathbf{k}(\mathbf{P}_{t+1}, \mathbf{P}_{t+1}) \end{bmatrix} \right) \quad (3)$$

and the probabilistic prediction of the next sample can be obtained by

$$\begin{aligned} f(\mathbf{P}_{t+1}) &\sim \mathcal{N}(\mu(\mathbf{P}_{t+1}), \sigma(\mathbf{P}_{t+1})) \\ \mu(\mathbf{P}_{t+1}) &= \mathbf{k}(\mathbf{P}_{t+1}, \mathbf{P}_{1:t}) \mathbf{K}(\mathbf{P}_{1:t}, \mathbf{P}_{1:t})^{-1} f(\mathbf{P}_{1:t}) \\ \sigma(\mathbf{P}_{t+1}) &= k(\mathbf{P}_{t+1}, \mathbf{P}_{t+1}) \\ &\quad - \mathbf{k}(\mathbf{P}_{t+1}, \mathbf{P}_{1:t}) \mathbf{K}(\mathbf{P}_{1:t}, \mathbf{P}_{1:t}) \mathbf{k}(\mathbf{P}_{1:t}, \mathbf{P}_{t+1}) \end{aligned} \quad (4)$$

This means that the mean for the unexplored pruning policy  $\mathbf{P}_{t+1}$  can be predicted via the history samples, and the corresponding variance of the prediction can also be obtained.

To enhance the sampling efficiency, a cheap surrogate function, which is called the acquisition function, is built to recommend the next sample point with the highest potential to maximize the objective function. EI (Mockus 1994; Brochu, Cora, and De Freitas 2010), which is defined by  $\mathbb{E}[\max(f(\mathbf{P}) - f(\mathbf{P}^+), 0)]$ , aims to find the sampling point that has the highest expected improvement over the current optimal policy, *i.e.*,  $\mathbf{P}^+$ , and has become one of the most popular acquisition functions over the past years. In this work, we utilize EI to sample the pruning policies.

The framework for the BO-based auto pruning scenario thus can be illustrated by the following Fig. 1. We first evaluate the randomly generated policies as the initial samples.

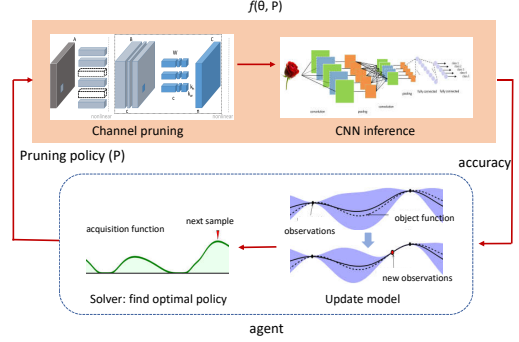


Figure 1: Solving the auto pruning problem by BO.

In this work, the initial policies are sampled according to the Sobol sequence (Joe and Kuo 2003, 2008), which is an evenly distributed quasi-random low dependency sequence and has an overwhelming advantage in providing stable and evenly distributed samples so that the later BO process can be more stable. Then, we build the Gaussian process model to estimate both the mean and the variance of the policies at unobserved locations according to equation 4. Next, the EI-based acquisition function is computed to indicate the potential of the benefits of each unexplored policy. Finally, the recommended policy, which shows the highest potential of obtaining a better pruned network, will be given by solving the maximum value of the acquisition functions, and will serve as the next sample to update the Gaussian process model. By repeating this process, the Gaussian model will become more and more accurate and the optimal pruning policy can be obtained during this process.

### 3.2 Bayesian Optimization with Clustering and Rollback

Though the BO-based agent has a high sampling efficiency, it is limited to low-dimensional problems. This is because the design space of auto pruning grows exponentially with the network depth. The computational workload for each sample will also increase significantly since the computational workload for the inverse of the matrix in equation 4 will grow significantly as more samples are collected. As a result, BO usually works efficiently for hyper-parameters less than ten (Li et al. 2016) and the high computation workload will make the BO-based auto pruning prohibitive when CNNs grow deeper.

The flow of our proposed BO framework is illustrated in Fig. 2. In this flow, a layer clustering algorithm is firstly employed to fuse the layers of the CNN model into clusters, and layers inside the same cluster will share the same pruning ratio. As a result, the design space can be significantly reduced and promising pruning policies can be found much more efficiently. Then, a low-dimensional Gaussian process model can be built to indicate the performance of the pruning policy, and an acquisition function is used to indicate the next sample which is similar to the naive BO process. However, note that the dimensions for our clustered BO problem

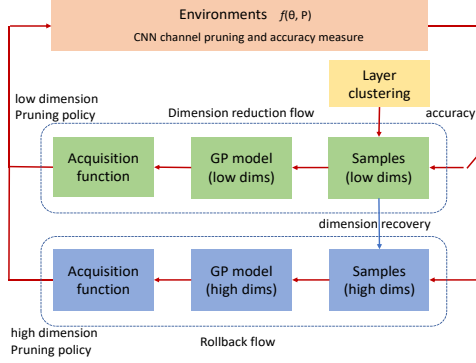


Figure 2: Bayesian optimization flow with clustering and rollback.

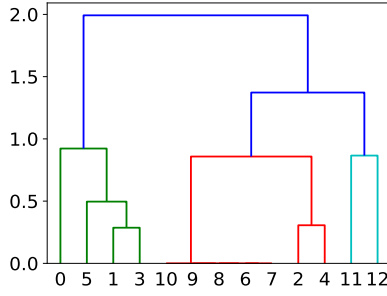


Figure 3: The dendrogram of layer clustering for MobileNetV1

are low, it can be computed much more efficiently. As the low-dimensional BO agent converges, the low-dimensional design space can be rolled back to high-dimensional spaces for a higher pruning accuracy. The low-dimensional samples can also be cast back to the high-dimensional space to build the Gaussian process model as priors. By combining the dimension reduction and rollback we found that the high-dimensional problem can be successfully solved and the BO-based auto pruning can be applied to very deep CNNs. In the following sections, we introduce our layer clustering algorithm and rollback algorithm in detail.

### 3.3 Layer Clustering

Our dimension reduction is based on agglomerative hierarchical clustering (Ward Jr 1963), which clusters the layers in a bottom-up manner. It can be illustrated by dendrogram, which shows the merging process and the intermediate clusters, as shown in Fig. 3.

To achieve layer clustering, we first select the features that can fully profile the layers. The number of input channels ( $n$ ), number of output channels ( $c$ ), and kernel size ( $k$ ) are included. In addition, we take the number of parameters and flops into account as they indicate how much redundancy a layer can have. We also include the size of the output feature map as a representative of the features extracted by the layer. Finally, we consider the quotient of  $n$  and  $c$  since it indicates the functionality of the layer.

Then, we define the distance between clusters in our auto pruning scenario according to Ward linkage, which aims to

### Algorithm 1: Bottom up clustering algorithm

---

```

Input:  $C, \mathbb{V}$ 
Result:  $\text{cluster}_{1:C}$ 
1  $n = N;$ 
2  $\text{cluster}_i = \{i\}_{i=1:N};$ 
3  $d^* = INF, \alpha = 1, \beta = 2;$ 
4 while  $n > C$  do
5   for  $i = 1 : n$  do
6     for  $j = i + 1 : n$  do
7       calculate  $d(\text{cluster}_i, \text{cluster}_j);$ 
8       if  $d < d^*$  then
9          $| d^* = d, \alpha = i, \beta = j$ 
10     $\text{cluster}_\alpha.\text{union}(\text{cluster}_\beta);$ 
11     $\text{delete}(\text{cluster}_\beta);$ 
12     $n = n - 1;$ 
13   $d^* = INF$ 

```

---

minimize the total within-cluster variance. We define the distance between cluster A and cluster B as:

$$d(A, B) = \frac{n_A n_B}{n_A + n_B} \sum_{v \in \mathbb{V}} \left( \frac{1}{n_A} \sum_i v_A^i - \frac{1}{n_B} \sum_i v_B^i \right)^2, \quad (5)$$

where  $v$  is the feature in the feature space  $\mathbb{V} = \{n, c, k, k\_out, \text{params}, \text{flops}, n/c\}$ ,  $n_A$  is the number of layers in cluster A,  $n_B$  is the number of layers in cluster B.

Then the layer clusters can be obtained according to Algorithm 1, where  $C$  indicates the number of clusters and  $\mathbb{V}$  is the features of each layer of the network to be pruned. The clustering can be achieved by merging the clusters with the shortest distance gradually until  $C$  is achieved, which can be specified by the users according to the dendrogram. In this work, different  $C$  are evaluated and analyzed in a comprehensive manner, as shown in the experiment section. As we observed, the numbers of clusters around eight have a similar performance and could be a preferred choice in most cases.

Our experiments show that although the design space for the clustering-based BO problem is significantly decreased, the performance we can achieve is comparable, or even superior to the naive BO algorithm. This is because the clustering-based BO is more time-efficient and thus leads to a higher probability of finding the high-performance pruning policies within the same time.

### 3.4 Roll Back for Higher Accuracy

Previously, we showed that the high-dimensional BO problem can be cast to a low-dimensional BO problem by the layer clustering algorithm and therefore high-performance pruning policies can be searched efficiently. However, the optimal pruning policy might be missed as we reduce the design space by sharing the pruning ratio within the same group. In this section, we show this potential performance loss can be avoided by rolling back to the high-dimensional space. We introduce our rollback algorithm from the following perspectives.

**When to roll back** In our algorithm, we roll back to the high-dimensional space after we collect enough informa-

tion during the low-dimensional BO process. More specifically, it mainly depends on two factors, which are the performance of the low-dimensional BO process, and the time-performance trade-off. For the first factor, we roll back when the low-dimensional BO converges. In our experiments, if the optimal pruning policies remain unchanged for more than 20 trials, we consider it has already reached its bottleneck and thus the rollback process can be conducted to search for better design points. On the other hand, we roll back when reaching the maximum trial, which is allowed for the consideration of timing efficiency. In our experiments, 100 trials turns out to be a good threshold to terminate the low-dimensional BO process and start the high-dimensional search to get a good trade-off between the timing efficiency and the accuracy of the pruned network. Too many trials for the low-dimensional space will achieve limited benefits to the high-dimensional space search but will cause a significantly increased workload, which is not necessarily needed.

**How to roll back** We roll back to the high-dimensional design space by firstly introducing a dimension recovery process for the samples. Being aware that the layer clusters, which are determined by the dendrogram, will remain unchanged during the BO process, we can map the low-dimensional samples back to high-dimensional space directly and build the high-dimensional Gaussian process model to explore the high-dimensional space. However, an alternative way, *i.e. gradual rollback*, is to recover the dimensions of the design space through a bridge stage, which indicates an intermediate design space between the low and high-dimensional design space. As shown in Fig. 3, our dimension reduction is achieved by hierarchical clustering which works by sequentially merging similar clusters. Therefore, it has a nice property that lower-level clusters in the dendrogram are consistent with the high-level clusters. As a result, we consider the intermediate clustering policy as the bridge stage, and the gradual rollback process is achieved by firstly rolling back to the bridge stage and then rolling back to the high-dimensional space.

Since the consistency of the hierarchical clustering can guarantee that the low-dimensional information can be effectively used as the prior knowledge for the searching in high-dimensional space, by doing this, we can effectively reduce the learning gap between the low and high-dimensional space, and the previous knowledge can be effectively utilized to guide the later searching process when the dimensionality is high.

**Searching domain after rolling back** To maintain the efficiency in high-dimensional searching and to take advantage of the visited data in low-dimensional space, we propose an adaptive searching domain scaling scheme, where we reduce the searching domain according to the searching history during the low-dimensional BO process. We store the past ten pruning policies with the highest pruning accuracy, *e.g.*,  $\mathbf{P}_j^{*i}$ , where  $i$  ranges from 1 to 10 and indicates the index of the high-performance samples in the buffer.  $j$  ranges from 1 to  $C$  and indicates the index of the clusters. Then, the searching region of the high-dimensional BO pro-

cess can be formulated as

$$\mathcal{D} = \left[ \min_{i,j} \mathbf{P}_j^{*i}, \max_{i,j} \mathbf{P}_j^{*i} \right]^C, \quad (6)$$

It can be observed that, in our framework, the searching domain of the high-dimensional BO is determined by the highest preservation ratio and the lowest counterpart in the top 10 history samples. By reducing the design space, the high-dimensional BO process can be conducted in a more efficient manner.

Our experiments show that our rollback algorithm will further improve the pruning accuracy, leading to more promising pruning policies which will not be discovered in the naive BO and the clustering-based BO.

## 4 EXPERIMENTS

In our experiments, we use GpyOpt (SheffieldML 2016) as the basic BO agent and implement the proposed methods base on it. RL agent in (He et al. 2018) is also implemented as a baseline. To make a fair comparison, we adopt the same channel pruning scheme with the RL counterpart. The accuracy is estimated based on a random subset of the training set, whose sizes are 5000 and 3000 for Cifar10 ILSVRC2012, respectively. We conduct our experiments on several representative CNN model architectures, including ResNet56 (He et al. 2016), MobileNetV1 (Howard et al. 2017), MobileNetV2 (Sandler et al. 2018) and VGG16 (Simonyan and Zisserman 2014). We run each experiment for 200 epochs, and we report the mean ( $m$ ) and the standard deviation ( $\sigma$ ) of 10 different runs. Our experiments are run on an Intel(R) Core(TM) i7-5820K CPU @3.30GHz with a Nvidia GeForce GTX TITAN X.

### 4.1 Experiments with ResNet56

ResNet56 is a representative model architecture trained on Cifar10 and it has a considerably large depth, leading to very high dimensions for layer-wise pruning tasks. Although the first layers of the residual branches are not prunable because the input feature maps are shared with the shortcut branches, there still remains 28 layers to be pruned, which will cause the curse of dimensionality problem for naive BO agent. As there are 3 blocks in ResNet56 and the structure of all layers within a block are the same, our clustering method sets each block as a cluster which is consistent with common sense. Therefore, there are only 3 parameters left for the BO agent to optimize.

In table 2, we list the mean value ( $m$ ) and the standard deviation  $\sigma$  of both top-1 and top-5 accuracy achieved by different methods when pruning 50% for ResNet56. Our proposed layer clustering method improves BO’s performance with 1.4% higher in top-1 accuracy. The rollback scheme further improves the accuracy by 0.9%. Note that in (He et al. 2018), the author claimed that AMC can achieve a 90.2% top1 accuracy in 400 epochs. For comparison, the best top1 accuracy of our proposed rollback method is up to 93.14 %, which is significantly higher than the result in (He et al. 2018).

method	top-1 $m$	top-1 $\sigma$	top-5 $m$	top-5 $\sigma$
RL	87.69	3.39	99.42	0.33
Original BO	90.29	1.63	99.72	0.11
Layer Clustering	91.68	0.43	99.77	0.06
Roll Back	92.53	0.56	99.86	0.05

Table 2: Performance for ResNet56.

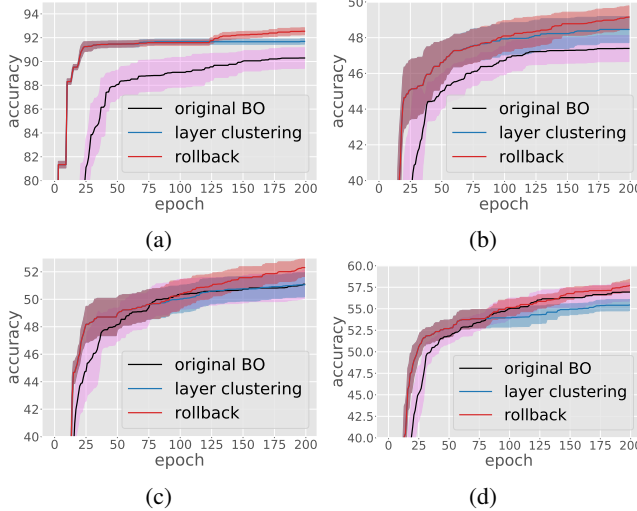


Figure 4: Comparison of BO-based methods for ResNet56 (a), MobileNetV1 (b), MobileNetV2 (c), VGG16 (d).

The table also shows that the BO agent outperforms RL in efficiency by a large margin. It can be observed that the BO-based searching scheme is more stable than the RL-based counterpart and converges much faster, as the  $\sigma$  of the RL agent is much higher than our proposed layer clustering and the rollback algorithm. In Fig. 4a, we show the effectiveness of the proposed methods in detail. The solid lines shown in the figure refer to the means, and the shaded areas refer to the corresponding  $\sigma$ . Obviously, the layer clustering method can significantly boost the convergence of the BO agent. After its convergence, the rollback scheme turns the design space back into a high-dimensional space and can further improve the accuracy of the pruned network.

Note that all methods take around 2300 seconds to finish 200 epochs, which indicates the time spent for each trial in BO and RL is close and the time overhead of rollback is ignorable. Thus, our method is also much more efficient from the perspective of wall clock time.

## 4.2 Experiments with MobileNetV1

MobileNetV1 is a popular single-branch network trained on ImageNet and it is known to be challenging to prune MobileNetV1 since it is designed to be highly compact. As the layers of MobileNet consist of pairs of depth-wise convolution and point-wise convolution layers, we only take the point-wise convolution layers into consideration when searching for the pruning policy, and the corresponding channels in the depth-wise layer will be removed accordingly. We also note that the first layer is not prunable as its channel should be in line with the input images, and simi-

method	top-1 $m$	top-1 $\sigma$	top-5 $m$	top-5 $\sigma$
RL	45.61	1.95	71.88	1.87
Original BO	47.39	1.39	73.11	1.47
Layer Clustering	48.46	1.39	74.17	1.31
Roll Back	49.15	1.19	74.61	1.15

Table 3: Performance for MobileNet V1

method	top-1 $m$	top-1 $\sigma$	top-5 $m$	top-5 $\sigma$
RL	43.15	5.45	69.84	5.01
Original BO	51.09	1.97	77.13	1.33
Layer Clustering	51.06	1.66	77.08	1.74
Roll Back	52.66	1.20	78.16	1.01

Table 4: Performance for MobileNetV2

larly for the final linear. As a result, there are 13 parameters for BO to optimize. We prune 50% flops for illustration purposes, and we divide the layers into 6 clusters.

In Table 3, we show the accuracy and corresponding  $\sigma$  for the proposed methods on MobileNetV1. Similar to the result of ResNet56, BO-based methods achieve significantly better results than the RL agent. Note that our rollback-based BO can achieve the best top-1 accuracy of 51.6%, and also outperforms the RL counterparts, which has an accuracy of 50.2%, as provided by AMC’s official webpage. Additionally, layer clustering-based BO outperforms the original BO agent by 1.07% in top-1 accuracy and 1.06% in top-5 accuracy. The rollback scheme further improves the accuracy by 0.7% and 0.5% in top-1 accuracy and top-5 accuracy, respectively. Note that we take only 3000 random images from Imagenet for evaluation, thus the  $\sigma$  is higher than that of the experiments on Cifar10 as expected.

In Fig. 4b, we compare the three BO-based methods in detail. Obviously, the layer clustering method speeds up the convergence of the BO agent significantly, based on which rollback scheme further improves the accuracy by returning the design space to high-dimensional space.

## 4.3 Experiments with MobileNetV2

We also test our method on the modern efficient network MobileNetV2, which is an improved version of MobileNetV1, and it is even more compact than MobileNetV1, making it more challenging to be pruned. It has a more complex structure than the aforementioned networks since it adopts an inverted residual structure while keeping the depth-wise and point-wise design in MobileNetV1. We use the same experimental setting as in Sec. 4.1 and 4.2 for the residual structure and the depth & point-wise structure, and there are 18 parameters for the BO agent to optimize. However, we divide the layers into 7 clusters since the number of layers in MobileNetV2 is more than that of MobileNetV1.

In Fig. 4c, we show the accuracy and corresponding  $\sigma$  for MobileNetV2. In contrast with the previous experiments, the layer clustering scheme fails to achieve better accuracy than naive BO. This makes sense as the similarity between layers is much lower in such a complex network, which increases the accuracy loss caused by layer clustering. However, the layer clustering scheme still boosts the convergence of BO at the beginning, as shown in Fig. 4c, although the benefits

method	top-1 $m$	top-1 $\sigma$	top-5 $m$	top-5 $\sigma$
RL	42.82	8.63	67.28	10.97
Original BO	56.94	2.00	81.91	1.51
Layer Clustering	55.43	1.24	80.71	0.99
Roll Back	57.70	1.36	82.39	1.05

Table 5: Performance for VGG16

rollback stage	top-1 $m$	top-1 $\sigma$	top-5 $m$	top-5 $\sigma$
12	52.21	1.48	77.81	1.34
13	52.31	1.23	77.98	1.07
14	52.25	1.07	78.02	1.26
15	52.66	1.20	78.16	1.01
16	52.17	1.20	77.80	1.05
17	51.97	1.73	77.66	1.53
direct	51.47	1.52	77.29	1.35

Table 6: Comparison of different rollback stage on MobileNetV2

diminish at around 75 epochs. This also motivates us to develop the rollback algorithm.

Table 4 and Fig. 4c together show the performance of our proposed rollback method. The experiments show that our rollback algorithm can raise the top-1 accuracy over the naive BO agent by 1.5% while achieving a lower  $\sigma$ . Moreover, our method consistently outperforms its RL-based counterpart by a large margin, as the RL agent needs much more time to converge.

#### 4.4 Experiments with VGG16

VGG is another popular single-branch network for image recognition and object detection. We conduct our experiments on the VGG16 model trained on ImageNet which consists of 13 convolutional layers and 3 fully connected layers. As the channel pruning method that we utilize is only suitable for convolutional layers, we skip the fully connected layers. We also skip the first layer for the aforementioned reason and there are 12 parameters for BO to optimize. In this experiment, we preserve 40% flops and divide the layers into 6 clusters.

As shown in Fig. 4d, the layer clustering scheme accelerates the optimization process at the beginning, but fails to achieve better accuracy than naive BO in the end. However, our proposed rollback method still achieves the best results, showing its good versatility. Table 5 shows more detailed information about our experiments on VGG16.

#### 4.5 Analysis of the cluster number

To compare the effect of  $C$ , we set  $C$  to different values and test each  $C$  for 5 times. Each time, we run 100 epochs since we only adopt layer clustering to speed up the searching and we do not focus on the converged performance of clustered BO.

Fig. 5a and Fig. 5b show the comparison between different  $C$  on MobileNetV1 and MobileNetV2. As we have claimed previously, the selected cluster numbers lead to similar performance. In experiments with MobileNetV1, although when the cluster number is six, the BO agent achieves a better result than others, the gap can be compensated after rollback. In experiments with MobileNetV2, the

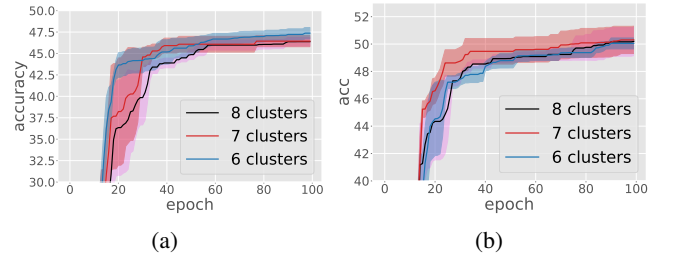


Figure 5: Comparison between different cluster numbers with MobileNetV1 (a) and MobileNetV2 (b).

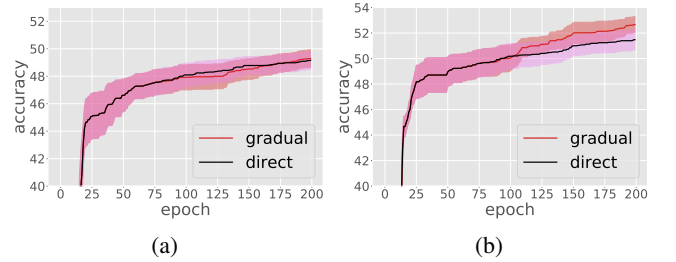


Figure 6: Comparison between direct rollback and gradual rollback with MobileNetV1 (a) and MobileNetV2 (b) (rollback to 9 and 15 clusters as bridge stage, respectively).

results of the selected cluster numbers are so close that the difference can be ignored.

#### 4.6 Gradual rollback for higher dimensionality

In this section, we demonstrate the effectiveness of the gradual rollback scheme. Fig. 6a and Fig. 6b show the comparison of the gradual and direct rollback on MobileNetV1 and MobileNetV2, respectively. When the total depth of a network is not too high, the direct rollback method is good enough to find the optimal policy. Therefore, gradual rollback shows little superiority in comparison with the direct rollback when pruning MobileNetV1. However, when the total depth gets higher, the performance of the BO agent decreases as the learning gap gets larger. In experiments on MobileNetV2, we set different  $C$  as the bridge stage of the gradual rollback to analyze its influence. As shown in Table 6, larger bridge clusters lead to larger learning gaps so that the performance decreases, while smaller bridge clusters fail to take advantage of the searching ability of BO. The experiments show that 15 clusters as the bridge stage achieves the best result. However, note that our proposed gradual rollback method consistently outperforms the direct rollback method.

### 5 Conclusion

In this paper, we proposed a novel layer clustering algorithm to prune the CNN models efficiently by sharing the preservation ratio among the same clusters. Then, we roll back the design space and further improve the accuracy of the pruning policy. Our experiments have validated the proposed layer-clustering and rollback-based BO algorithm. In the future, we would like to extend our work to auto quantization and auto network architecture search.

## References

Brochu, E.; Cora, V. M.; and De Freitas, N. 2010. A tutorial on Bayesian optimization of expensive cost functions, with application to active user modeling and hierarchical reinforcement learning. *arXiv preprint arXiv:1012.2599* .

Chen, C.; Tung, F.; Vedula, N.; and Mori, G. 2018. Constraint-aware deep neural network compression. In *Proceedings of the European Conference on Computer Vision (ECCV)*, 400–415.

Han, S.; et al. 2015. Learning both weights and connections for efficient neural network. In *Advances in neural information processing systems*.

He, K.; Zhang, X.; Ren, S.; and Sun, J. 2016. Deep residual learning for image recognition. In *Proceedings of the IEEE conference on computer vision and pattern recognition*, 770–778.

He, Y.; et al. 2017. Channel pruning for accelerating very deep neural networks. In *Proceedings of the IEEE ICCV*.

He, Y.; et al. 2018. AMC: AutoML for model compression and acceleration on mobile devices. In *Proceedings of the ECCV*, 784–800.

Howard, A. G.; Zhu, M.; Chen, B.; Kalenichenko, D.; Wang, W.; Weyand, T.; Andreetto, M.; and Adam, H. 2017. Movenets: Efficient convolutional neural networks for mobile vision applications. *arXiv preprint arXiv:1704.04861* .

Joe, S.; and Kuo, F. Y. 2003. Remark on algorithm 659: Implementing Sobol’s quasirandom sequence generator. *ACM Transactions on Mathematical Software (TOMS)* 29(1): 49–57.

Joe, S.; and Kuo, F. Y. 2008. Constructing Sobol sequences with better two-dimensional projections. *SIAM Journal on Scientific Computing* 30(5): 2635–2654.

Krizhevsky, A.; Sutskever, I.; and Hinton, G. E. 2012. Imagenet classification with deep convolutional neural networks. *Advances in neural information processing systems* 25: 1097–1105.

Li, C.-L.; Kandasamy, K.; Póczos, B.; and Schneider, J. 2016. High dimensional Bayesian optimization via restricted projection pursuit models. In *Artificial Intelligence and Statistics*, 884–892. PMLR.

Lillicrap, T. P.; et al. 2015. Continuous control with deep reinforcement learning. *arXiv preprint arXiv:1509.02971* .

Louizos, C.; et al. 2017. Learning Sparse Neural Networks through  $L_0$  Regularization. *arXiv preprint arXiv:1712.01312* .

Ma, X.; Triki, A. R.; Berman, M.; Sagonas, C.; Cali, J.; and Blaschko, M. B. 2019. A bayesian optimization framework for neural network compression. In *Proceedings of the IEEE/CVF International Conference on Computer Vision*, 10274–10283.

Mockus, J. 1994. Application of Bayesian approach to numerical methods of global and stochastic optimization. *Journal of Global Optimization* 4(4): 347–365.

Mockus, J.; and Mockus, L. 1991. Bayesian approach to global optimization and application to multiobjective and constrained problems. *Journal of optimization theory and applications* 70(1): 157–172.

Mockus, J.; Tiesis, V.; and Zilinskas, A. 1978. The application of Bayesian methods for seeking the extremum. *Towards global optimization* 2(117-129): 2.

Sandler, M.; Howard, A.; Zhu, M.; Zhmoginov, A.; and Chen, L.-C. 2018. Mobilenetv2: Inverted residuals and linear bottlenecks. In *Proceedings of the IEEE conference on computer vision and pattern recognition*, 4510–4520.

SheffieldML. 2016. GPyOpt: A Bayesian optimization framework in python. *Github* [Http://github.com/SheffieldML/GPyOpt](http://github.com/SheffieldML/GPyOpt).

Simonyan, K.; and Zisserman, A. 2014. Very deep convolutional networks for large-scale image recognition. *arXiv preprint arXiv:1409.1556* .

Tung, F.; Muralidharan, S.; and Mori, G. 2017. Fine-pruning: Joint fine-tuning and compression of a convolutional network with Bayesian optimization. *arXiv preprint arXiv:1707.09102* .

Wang, K.; et al. 2019. HAQ: Hardware-Aware Automated Quantization with Mixed Precision. In *Proceedings of the IEEE Conference on CVPR*, 8612–8620.

Wang, Z.; Zoghi, M.; Hutter, F.; Matheson, D.; De Freitas, N.; et al. 2013. Bayesian Optimization in High Dimensions via Random Embeddings. In *IJCAI*, 1778–1784.

Ward Jr, J. H. 1963. Hierarchical grouping to optimize an objective function. *Journal of the American statistical association* 58(301): 236–244.

Zhuang, Z.; et al. 2018. Discrimination-aware channel pruning for deep neural networks. In *Advances in Neural Information Processing Systems*.